Published in final edited form as:
Biochem Biophys Res Commun. 2008 February 22; 366(4): 1081–1088.

Upstream open reading frames regulate the expression of the nuclear Wnt13 isoforms

Tao Tang, **Kyle Rector**, **Corey D. Barnett**, and **Catherine D. Mao**
Graduate Center for Nutritional Sciences, University of Kentucky, Lexington, KY 40506

Abstract

Wnt proteins control cell survival and cell fate during development. Although Wnt expression is tightly regulated in a spatio-temporal manner, the mechanisms involved both at the transcriptional and translational levels are poorly defined. We have identified a downstream translation initiation codon, AUG(+74), in Wnt13B and Wnt13C mRNAs responsible for the expression of Wnt13 nuclear forms. In this report, we demonstrate that the expression of the nuclear Wnt13C form is translationaly regulated in response to stress and apoptosis. Though the 5'-leaders of both Wnt13C and Wnt13B mRNAs have an inhibitory effect on translation, they did not display an internal ribosome entry site activity as demonstrated by dicistronic reporter assays. However, mutations or deletions of the upstream AUG(−99) and AUG(+1) initiation codons abrogate these translation inhibitory effects, demonstrating that Wnt13C expression is controlled by upstream open reading frames. Since long 5'-untranslated region with short upstream open reading frames characterize other Wnt transcipts, our present data on the translational control of Wnt13 expression open the way to further studies on the translation control of Wnt expression as a modulator of their subcellular localization and activity.

Introduction

Wnt proteins play a key role during development by controlling cell survival, proliferation and differentiation [1]. There are 19 different Wnt genes in mammals and their expression is tightly regulated in a spatio-temporal manner during development in particular via tissue specific transcriptional control [1]. However, increasing evidence suggests that numerous developmental and apoptosis factors also regulated at the translational level to ensure fine tuning of expression during the early stages of development and regulated cell death [2,3].

Internal ribosome entry segment (IRES) is the most common mechanism for alternative translation initiation in particular during apoptosis and the expression of numerous anti-or pro-apoptotic factors is controlled by an IRES-dependent and cap-independent mechanism [4,5]. IRES involves specific RNA secondary structures such as stem loop structures able to recruit IRES translation accessory factors (ITAFs) that drive translation initiation from the alternative AUG codon [5,6]. In the Wnt signaling pathways, only the expression of LEF-1, a downstream effector of the Wnt/β-catenin signaling pathway, was shown to be controlled by both alternative promoter and IRES, which result in the expression of the full-length and β-catenin responsive LEF-1 form particularly in tumoral cells [7,8]. In addition to IRES, other mechanisms such as leaky ribosome scanning, ribosome shunting, and ribosome re-initiation seem to occur more often than at first suspected [9]. All these mechanisms including IRES are regulated either

Correspondence to: Dr. Catherine D. Mao, Fax: (859)-257-3646, e-mail: cdmao2@uky.edu.

positively or negatively by the translation of short upstream open reading frames (ORFs) [10,11].

The complexity of Wnt gene expression has begun to be unraveled in different species with the identification of alternative promoters such as in human *wnt13* [12,13] and *wnt16* [14] genes, which are responsible for the expression of Wnt proteins differing in their N-terminal sequences [12–14] and in their sub-cellular localizations [12]. In addition to two alternative promoters giving rise to either Wnt13A mRNA or Wnt13B and Wnt13C mRNAs, Wnt13 expression is also controlled by alternative splicing and alternative translation initiation sites [12]. Indeed, we have recently shown that although Wnt13B and Wnt13C mRNAs differ by an alternative skipping of exon 2 (see Fig. 1A), in both cases, a downstream translation start site, AUG(+74), was used leading to the expression of the nuclear S-Wnt13B/Wnt13C forms associated in endothelial cells with an increased susceptibility to TNFα-induced apoptosis [12]. In this study, our goal was to investigate the regulation and the mechanisms involved in the choice of the translation start site AUG(+74) giving rise to the nuclear S-Wnt13B and Wnt13C forms.

Material and Methods

Materials

Lipolysaccharide (LPS) and tumor necrosis factor (TNF-α) were from Calbiochem. LY294002, tunicamycin, MG132, and ALLN were purchased from Sigma (St-Louis, MO, USA). The specific proteasome inhibitors epoxomycin and eponomycin were a kind gift from Dr. Kim (University of Kentucky). The rabbit polyclonal antibodies against D175-cleaved-caspase 3, caspase 3, β-actin, and the secondary horseradish peroxidase-conjugated antibodies were purchased from Cell Signaling Technology (Danvers, MA). The rabbit polyclonal anti-Flag tag antibodies were obtained from Cayman-Chemicals (Ann Arbor, MI).

Cells and transfections

The primary BAEC (Cambrex) were maintained in DMEM 1g/L glucose with 5% FBS and the HEK293T cell line (Invitrogen, Carlsbad, CA) was maintained in DMEM 4.5g/L glucose with 10% FBS. Both media were supplemented with penicillin and streptomycin. Transfections were performed with Exgene500 reagent accordingly to the manufacturer's recommendations (Fermentas).

Wnt13C-Flag and Wnt13B-Flag expression plasmids

The Wnt13B-Flag and Wnt13C-Flag expression constructs were previously described as well as the mutated M1L-Wnt13B-Flag, M1L-Wnt13C-Flag and M74L-Wnt13B-Flag constructs [12]. The pΔCMV-Wnt13B-Flag construct with the deletion of the CMV promoter sequences was obtained from the pCR3-Wnt13B-Flag construct by restriction digest with *Spe1*. The insertion of the Myc-tag sequence at the AUG1 codon of Wnt13C was done by PCR using the primers 5'-CCACCATGGGCGAACAAAAACTCATCTCAGAAGAGGATCTGGTGTTGGATGGCCTTG-3' and 5'-TCACTTATCGTCGTCATCCTTGTAATCTGCGGTCTGGTCCAGCCAC-3'. The deletion mutants Δ12- and Δ17-Wnt13B, where the first 12 and 17 AAs respectively were deleted meanwhile a start codon with upstream consensus Kozak sequences (CCACCatg) [15] were added in frame, were also generated by PCR with the common reverse primer 5'-TCACTTATCGTCGTCATCCTTGTAATCTGCGGTCTGGTCCAGCCAC-3' and the specific forward primers 5'-GCCACCATGTTTGGAATTCTTCAAAAACTG-3' (Δ12-Wnt13B-Flag) and 5'- GCCACCATGAAAACTGAAGGATCCTTG-3' (Δ17-Wnt13B-Flag).

Reverse transcription-PCR and real-time PCR analyses

Total RNA extraction were performed using Trizol reagent (Invitrogen). Total RNA (1 μg) was subjected to DNAse I treatment for 15 min (Invitrogen) prior to being reverse transcribed with 0.5 μg oligo dT and 200U reverse transcriptase (Invitrogen). For the RT controls, the reverse transcriptase was omitted. Real-time PCRs were performed in duplicates, with an equivalent of 16 ng total RNA per reaction and 10 pmoles of either Wnt13 primers: 5'-CTTGGAGTGGTAGCCATAAGC-3'/5'-GCATGATGTCTGGGTAACGC-3' or rpL30 primers for normalization: 5'-CTCAACGAGAACAAGCTATC-3'/5'-CCAATCTGCCGACTTAGCG-3', using the SyBr Green PCR core reagent and the ABI7000 apparatus (Applied-Biosystems, Forest City, CA, USA).

Whole cell extracts and Western Blot analysis—After washes with cold PBS, the cells were lysed in 50 mM HEPES pH 7.4, 0.1% CHAPS, 5 mM DTT and 2 mM EDTA supplemented with protease and phosphatase cocktail inhibitors (Sigma). Equal amounts of proteins were denaturated, fractionated on SDS-polyacrylamide gels (PAGE) and transferred onto Immobilon P membrane. After blocking, the membranes were incubated with the various primary antibodies as indicated and subsequently with the appropriate secondary antibodies conjugated to horseradish peroxidase. Immuno-reactive proteins were detected using SuperSignal® chemiluminescence (Pierce Chemical Co, Rockford, IL, USA) and the intensity of the resulting bands was determined by densitometry using Scion software.

Dicistronic Renilla Luciferase (RL)-Firefly Luciferase (FL) constructs and dual luciferase assays—The 5' leaders of human Wnt13B and Wnt13C mRNAs were amplified by RT-PCR from HUVEC total RNAs using the primers 5'-CCCTGAAGAGCCCAAGCAATG-3' and 5'-GCATGATGTCTGGGTAACGCTG-3', and cloned into pGEM-T-Easy (Promega). These 5' leaders include the common 5'-UTR sequence and the alternative exon 2 between the two alternative translation start sites (Fig. 1A). The Wnt13B and Wnt13C leader sequences were subcloned either upstream of the RL coding sequence in the pRL-HCV-IRES-FL construct to test their inhibitory effects on RL translation or in the intercistronic space of the pRL-null-FL construct to test their IRES activities. The pRL-HCV-FL and pRL-ECMV-FL constructs containing the IRES of HCV and ECMV respectively were a kind gift from. Dr. Kruger and previously described [16]. The pRL-null-FL construct was generated from the pRL-HCV-FL by deletion of the HCV-IRES and insertion of the SacII-XbaI sites for subsequent subcloning of the various Wnt13B and Wnt13C leader sequences. BAEC and HEK293T cells were co-transfected with 5 ng of pCMV-β-galactosidase construct for normalization purposes and with 250 ng of the various pRL-FL constructs for 24 h prior to being treated with 1 μM MG132 for 10 h. Cells were then harvested, lysed and assayed for RL and FL activities using the dual-luciferase assays (Promega) and for β-galactosidase activities with Galacto Light Plus (Tropix-Applied Biosystems) on an LmaxII luminometer (Molecular Devices). The ratio RL/FL and RL/β-galactosidase were determined to assess the translation inhibitory activity of Wnt13 5'-leader sequences while the ratio FL/RL, FL/β-galactosidase and RL/β-galactosidase were determined to assess the IRES activity of Wnt13 5'-leader sequences. At least three independent transfection experiments were performed in duplicates.

Results and Discussion

The 5'-leader sequences of Wnt13B and Wnt13C mRNAs are highly structured

We have previously shown that two alternative initiation start sites, AUG(+1) and AUG(+74), were used during the translation of Wnt13B and Wnt13C mRNAs generating the mitochondrial L-Wnt13B and the nuclear Wnt13C/S-Wnt13B forms (Fig. 1) and [12]. The 5'-leader sequences of both Wnt13B and Wnt13C mRNAs present several features associated with

regulated translation initiation [6]. Indeed, the 5'-UTRs are rather long, with 120 nucleotides before the initiation codon AUG(+1) and with either 340 or 229 nucleotides before the initiation codon AUG(+74) in Wnt13B and Wnt13C mRNAs respectively (Fig. 1A). There are also an additional uORF close to the 5'-end starting at AUG(−99) and several possibilities of CUG initiation codon including one in frame with AUG(+1) in the longest 5'-UTR reported so far [13]. None of these initiation codons are in an optimum Kozak environment, but both AUG (−99) and AUG(+74) present an A/G nucleotide in position −2 and thus appear in a more favorable environment than AUG(+1) [15]. Based on M-fold analysis [17], Wnt13B and Wnt13C 5'-mRNA leader sequences display highly stable secondary structures with free energies ΔG ranging from −88 to −104 kcal/mole in Wnt13B mRNA and from to −70 to −75 kcal/mole in Wnt13C mRNA [17], which are known to impede ribosome scanning [6,11]. Moreover, using rapid amplification of cDNA 5'-end we found that the longest Wnt13C cDNA in HUVEC started at the nucleotide +75 of the reported sequence (not shown), and was thus devoid of the uAUG(−99) and uORF and is represented by Wnt13C-Flag and Wnt13B-Flag constructs in our study. These data also indicated the possibility of different transcription start sites generating Wnt13B and Wnt13C mRNA leaders with various lengths, structures and uORFs, which is also a regulatory feature common to various growth factors including TGFβ [3,11].

Modifications of the sequences surrounding AUG1 alter the expression of Wnt13B and Wnt13C

To further ascertain that the translation from the downstream start codon AUG(+74) resulting in the expression of the nuclear S-Wnt13B and Wnt13C forms was not due to the presence of a cryptic promoter located in the 5'-mRNA leader sequences, the CMV promoter in pCR3-Wnt13B-Flag construct was deleted to generate the pΔCMV-Wnt13B-Flag construct. As previously described [12], the transfection of pCR3-Wnt13B-Flag construct in HEK293 cells resulted in the appearance of the L-Wnt13B and S-Wnt13B doublet, while the transfection of pCR3-Wnt13C and pCR3-M1L-Wnt13B gave rise to the short form and transfection of pCR3-M74L-Wnt13B resulted in the expression of the long form (Fig. 1B). In contrast, the transfection of pΔCMV-Wnt13B-Flag construct resulted in the total absence of expression of Wnt13-Flag mRNAs (not shown) and of Flag-tagged proteins (Fig. 1B), confirming the presence of the alternative translation start sites AUG(+1) and AUG(+74) in Wnt13B and Wnt13C mRNAs. To determine the requirement for RNA structures and/or sequences in this downstream translation initiation, Wnt13B-Flag expression constructs were generated with deletions of the sequences corresponding to the first 12 AAs and 17AAs and with the insertion instead of an initiation codon in a consensus gccaccAUG Kozak sequence [15] (Fig. 1A). Surprisingly, the Δ12-Wnt13B-Flag construct resulted in a barely detectable expression from both the inserted AUG(+12) and the downstream AUG(+74), while the Δ17-Wnt13B-Flag construct resulted in the expression mainly from the inserted AUG(+17) (Fig. 1B). On the other hand, modification of AUG(+1) with the insertion of a myc-tag sequence in Wnt13C, which should affect only the expression of the short ORF, resulted also in a dramatic decrease of the expression from the downstream AUG(+74) (Fig. 1B). Together these results indicated that the RNA sequences and/or structures around the AUG(+1) were critical for the translation initiation at the downstream AUG(+74) both in Wnt13B and Wnt13C mRNAs.

The expression of Wnt13C form increased in response to stress and apoptosis inducers

However, the expression of Wnt13C was always lower than its equivalent S-Wnt13B both in primary BAEC and transformed HEK293 cells (Fig. 1B). These differences occurred in absence of significant differences in levels of the exogenous Wnt13B-Flag and Wnt13C-Flag mRNAs as determined by real-time PCR (not shown) indicating that the translation of Wnt13C was inefficient as compared to S-Wnt13B translation although the same downstream AUG (+74) was used. Next, we determined whether the use of the downstream AUG(+74) initiation

codon was regulated during apoptosis using the apoptosis-sensitive primary BAEC. As shown in Fig. 2B, the expression of Wnt13C in BAEC was increased by different stress and apoptosis inducers including all the inhibitors of the proteasome tested, ALLN, MG132, epoxomycin and eponomycin, the inflammatory and apoptotic inducers TNFα and LPS, and the PI3kinase inhibitor LY294002 (Fig. 2B). The levels of Wnt13C expression correlated with the appearance of cleaved-caspase 3, though the proteasome inhibitors were inducing higher levels of Wnt13C (20 fold) than LPS treatment (4 fold) (Fig. 2B). Nonetheless, a sole increase of Wnt13C-Flag stability triggered by the proteasome inhibitors was incompatible with the facts that S-Wnt13B, the equivalent of Wnt13C, was observed in BAEC in absence of treatment (Fig. 2A) and that the expression of both Wnt13B and Wnt13C was dependent on RNA sequences and/or structures (Fig. 1B). Also, these differences in Wnt13C-Flag expression could not be explained by the sole 1.5 fold increase in the exogenous Wnt13C-Flag mRNA levels after MG132 treatment as determined by real-time PCR (Fig. 2C). The analysis of the PCR products on agarose gels confirmed the absence of spurious splicing of the exogenous Wnt13B-Flag and Wnt13C-Flag mRNAs even after MG132 treatment (Fig. 2C). On the other hand, proteasome inhibition was shown to affect translation at different levels including by increasing the activity of the initiation factors eIF2 and eIF4E and thus the translation of stress related factors [18, 19]. Taken together these data indicated that Wnt13C expression was regulated at the translational level in particular by stress and apoptosis inducers and thus suggested the possibility of the presence of an IRES within Wnt13C mRNA.

The 5’-leader sequences of Wnt13B and Wnt13C mRNAs do not behave like an IRES

To test the presence of an IRES within Wnt13B and Wnt13C mRNAs, the 5’-leader sequences were inserted in the pRL-Null-FL dicistronic vector between the coding sequences of *renilla* luciferase (RL) and firefly luciferase (FL) with Wnt13 AUG(+74) in frame with the FL initiation codon (Fig. 3A). In primary BAEC, only the positive control pRL-ECMV-FL displayed significant levels of FL activities, while the transfection of the pRL-Null-FL, pRL-5’-Wnt13B-FL and pRL-5’-Wnt13C-FL resulted in undetectable levels of FL activities (not shown). In HEK293 cells, though the FL activities were detected after transfection of all the dicistronic constructs, the presence of Wnt13B and Wnt13C 5’-UTR sequences did not increase the expression of FL but instead decreased it as compared with the negative control pRL-Null-FL (Fig. 3B) resulting in FL levels representing less than 0.1% of the RL levels. In contrast, the levels of FL activities represented 17% of the RL activities in HEK293 transfected with the IRES-positive control pRL-ECMV-FL (Fig. 3B). Moreover, treatment with 1 μM MG132 had no significant effects on the levels of FL activities including in cells expressing the IRES-positive construct pRL-ECMV-FL (Fig. 3B). These results ruled out the presence of an IRES within both Wnt13B and Wnt13C 5’-leader sequences and also suggested that these 5’-leaders had rather an inhibitory activity on translation consistent with their stable secondary structures. In agreement with this inhibitory effect, deletion of the Wnt13B 5’-UTR sequences up to 7 nucleotides upstream of AUG(+1), resulted in levels of FL activities similar as the negative control pRL-Null-FL (Fig. 3B).

The upstream ORFs decrease the efficiency of translation of Wnt13B and Wnt13C mRNAs

To further test the inhibitory activity of Wnt13B and Wnt13C 5’-leaders on translation, they were inserted upstream of the RL reporter sequence with the AUG(+74) in frame with the RL initiation codon (Fig. 4A). The expression of RL was significantly inhibited up to 75% and 70% by Wnt13B 5’-leader and, 95% and 85% by Wnt13C 5’-leader in BAEC and HEK293 cells respectively (Fig. 4A). Treatment with 1 μM MG132 had no significant effect on this inhibitory effect after normalization (Fig. 4A). Since the presence of uORFs alters the efficiency of translation and Wnt13C-leader contains two uORFs instead of one in Wnt13B-leader, we tested the effects of variable numbers of uORFs in Wnt13C leaders on the expression of Wnt13C. As shown in Fig. 4B, Wnt13C expression was increased gradually by the sequential

deletion of uAUG(−99) and mutation of AUG(+1). Similar increase of S-Wnt13B expression was observed by the deletion and/or mutation of the uAUG(−99) and AUG(+1). These results demonstrated that the uORFs were mainly responsible for the inhibitory activities of Wnt13B and Wnt13C 5'-leaders on the expression of Wnt13 nuclear forms. Nonetheless, independently of the number of uORFs and in absence of significant differences in the levels of mRNAs (not shown), the expression of Wnt13C constructs was always lower than the corresponding Wnt13B constructs indicating that the presence of exon 2 sequences enhances the translation initiation from the AUG(+74) codon. Moreover, they indicated that the AUG(+74) was also the major initiation codon in Wnt13B mRNA accordingly to the respective strength of the AUG (+74) and AUG(+1) initiation codons.

In conclusion, our data demonstrate that the expression of the nuclear Wnt13C and S-Wnt13B forms from the initiation codon AUG(+74) is negatively controlled by uORFs within the 5'-leader sequences. Although the expression of Wnt13C was increased by stress and apoptosis inducers and the initiation from AUG(+74) was favored by the presence of exon-2 sequences and of RNA sequence and/or structure surrounding the AUG(+1) codon, there was no evidence for the presence of an IRES driving the translation initiation from the AUG(+74) codon. These long 5'-leaders containing several uORFs are not unique to human Wnt13B/C transcripts but are in fact well conserved in most of Wnt transcripts (Table 1), suggesting that Wnts like other growth factors and potent cell regulators might be tightly regulated also at the translational level via in particular differential uORFs.

Acknowledgements

We are thankful to Drs. Martin Kruger and Kyung-Bo Kim for the kind gifts of the pRL-HCV-FL and pRL-ECMV-FL constructs and of epoxomycin and eponomycin compounds respectively. This work was supported by NIH grant HL68698 to C.D.M.

References

1. Moon RT, Brown JD, Torres M. WNTs modulate cell fate and behavior during vertebrate development. Trends Genet 1997;13:157–162. [PubMed: 9097727]
2. van der Velden AW, Thomas AA. The role of the 5' untranslated region of an mRNA in translation regulation during development. Int. J. Biochem. Cell. Biol 1999;31:87–106. [PubMed: 10216946]
3. Willis AE. Translational control of growth factor and proto-oncogene expression. Int. J. Biochem. Cell Biol 1999;31:73–86. [PubMed: 10216945]
4. Holcik M, Sonenberg N. Translational control in stress and apoptosis. Nat. Rev. Mol. Cell. Biol 2005;6:318–327. [PubMed: 15803138]
5. Spriggs KA, Bushell M, Mitchell SA, Willis AE. Internal ribosome entry segment-mediated translation during apoptosis: the role of IRES-trans-acting factors. Cell Death Differ 2005;12:585–591. [PubMed: 15900315]
6. Stoneley M, Willis AE. Cellular internal ribosome entry segments: structures, trans-acting factors and regulation of gene expression. Oncogene 2004;23:3200–3207. [PubMed: 15094769]
7. Jimenez J, Jang GM, Semler BL, Waterman ML. An internal ribosome entry site mediates translation of lymphoid enhancer factor-1 RNA. RNA 2005;11:1385–1399. [PubMed: 16120831]
8. Hovanes K, Li TW, Munguia JE, Truong T, Milovanovic T, Lawrence Marsh J, Holcombe RF, Waterman ML. Beta-catenin-sensitive isoforms of lymphoid enhancer factor-1 are selectively expressed in colon cancer. Nat. Genet 2001;28:53–57. [PubMed: 11326276]
9. Kozak M. A second look at cellular mRNA sequences said to function as internal ribosome entry sites. Nucleic Acids Res 2005;33:6593–6602. [PubMed: 16314320]
10. Yaman I, Fernandez J, Liu H, Caprara M, Komar AA, Koromilas AE, Zhou L, Snider MD, Scheuner D, Kaufman RJ, Hatzoglou M. The zipper model of translational control: a small upstream ORF is the switch that controls structural remodeling of an mRNA leader. Cell 2003;113:519–531. [PubMed: 12757712]

11. Meijer HA, Thomas AA. Control of eukaryotic protein synthesis by upstream open reading frames in the 5'-untranslated region of an mRNA. Biochem. J 2002;367:1–11. [PubMed: 12117416]
12. Struewing IT, Toborek A, Mao CD. Mitochondrial and nuclear forms of Wnt13 are generated via alternative promoters, alternative RNA splicing, and alternative translation start sites. J. Biol. Chem 2006;281:7282. [PubMed: 16407296]
13. Katoh M, Kirikoshi H, Saitoh T, Sagara N, Koike J. Alternative splicing of the WNT-2B/WNT-13 gene. Biochem. Biophys. Res. Commun 2000;275:209–216. [PubMed: 10944466]
14. Fear MW, Kelsell DP, Spurr NK, Barnes MR. Wnt-16a, a novel Wnt-16 isoform, which shows differential expression in adult human tissues. Biochem. Biophys. Res. Commun 2000;278:814–820. [PubMed: 11095990]
15. Kozak M. An analysis of 5'-noncoding sequences from 699 vertebrate messenger RNAs. Nucleic Acids Res 1987;15:8125–8148. [PubMed: 3313277]
16. Kruger M, Beger C, Welch PJ, Barber JR, Manns MP, Wong-Staal F. Involvement of proteasome alpha-subunit PSMA7 in hepatitis C virus internal ribosome entry site-mediated translation. Mol. Cell. Biol 2001;21:8357–8364. [PubMed: 11713272]
17. Zuker M. Mfold web server for nucleic acid folding and hybridization prediction. Nucleic Acids Res 2003;31:3406–3415. [PubMed: 12824337]
18. Murata T, Shimotohno K. Ubiquitination and proteasome-dependent degradation of human eukaryotic translation initiation factor 4E. J. Biol. Chem 2006;281:20788–20800. [PubMed: 16720573]
19. Cowan JL, Morley SJ. The proteasome inhibitor, MG132, promotes the reprogramming of translation in C2C12 myoblasts and facilitates the association of hsp25 with the eIF4F complex. Eur. J. Biochem 2004;271:3596–3611. [PubMed: 15317596]

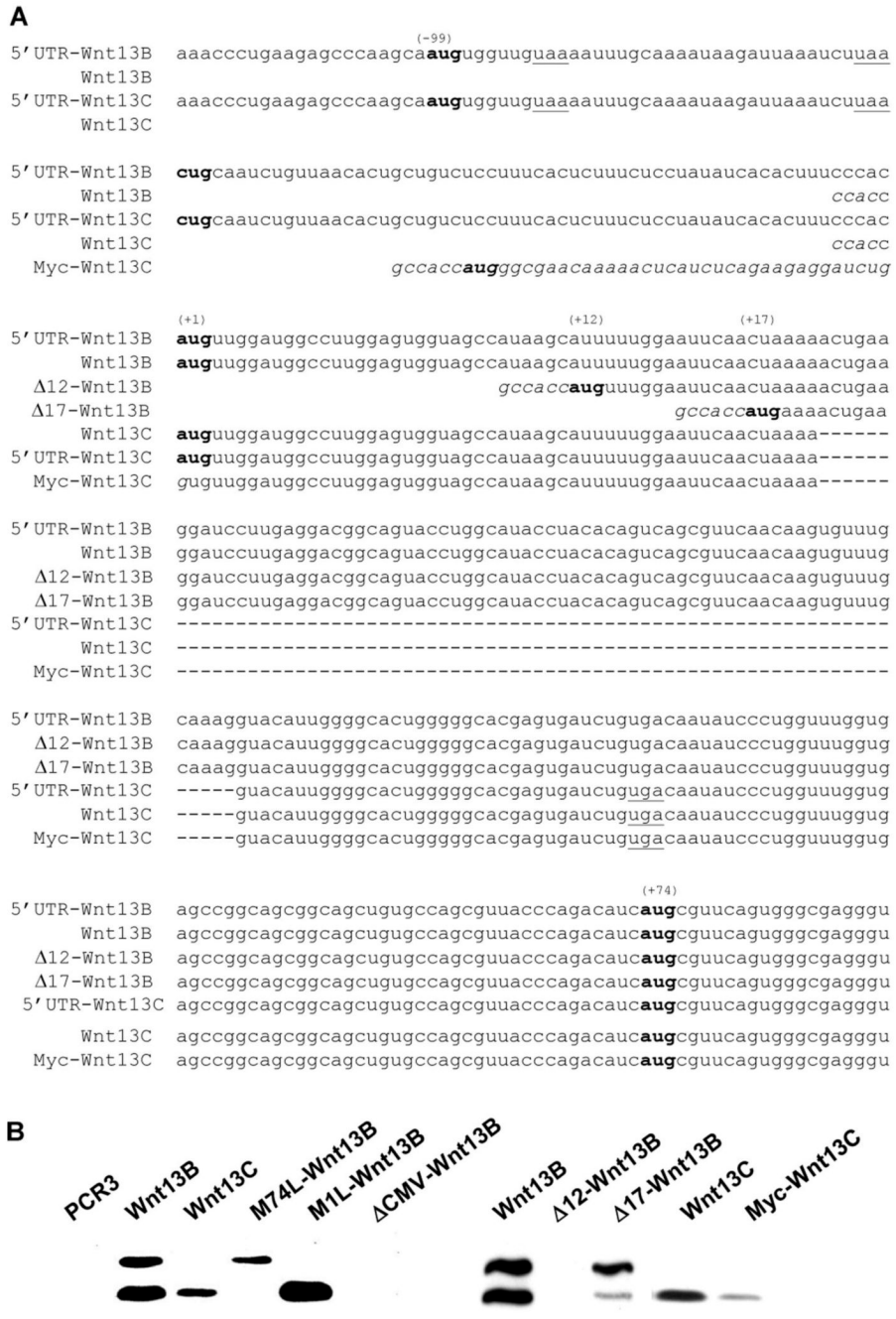

Figure 1.

A) Alignment of Wnt13B and Wnt13C 5'-leader sequences. The putative translation start sites AUG and CUG are indicated in bold and numbered. The premature stop codons are underlined. The different Wnt13 expression constructs used in this study are indicated. B) Western blot analysis of Wnt13B-Flag and Wnt13C-Flag expression in HEK293 cells transiently transfected for 36 h as indicated.

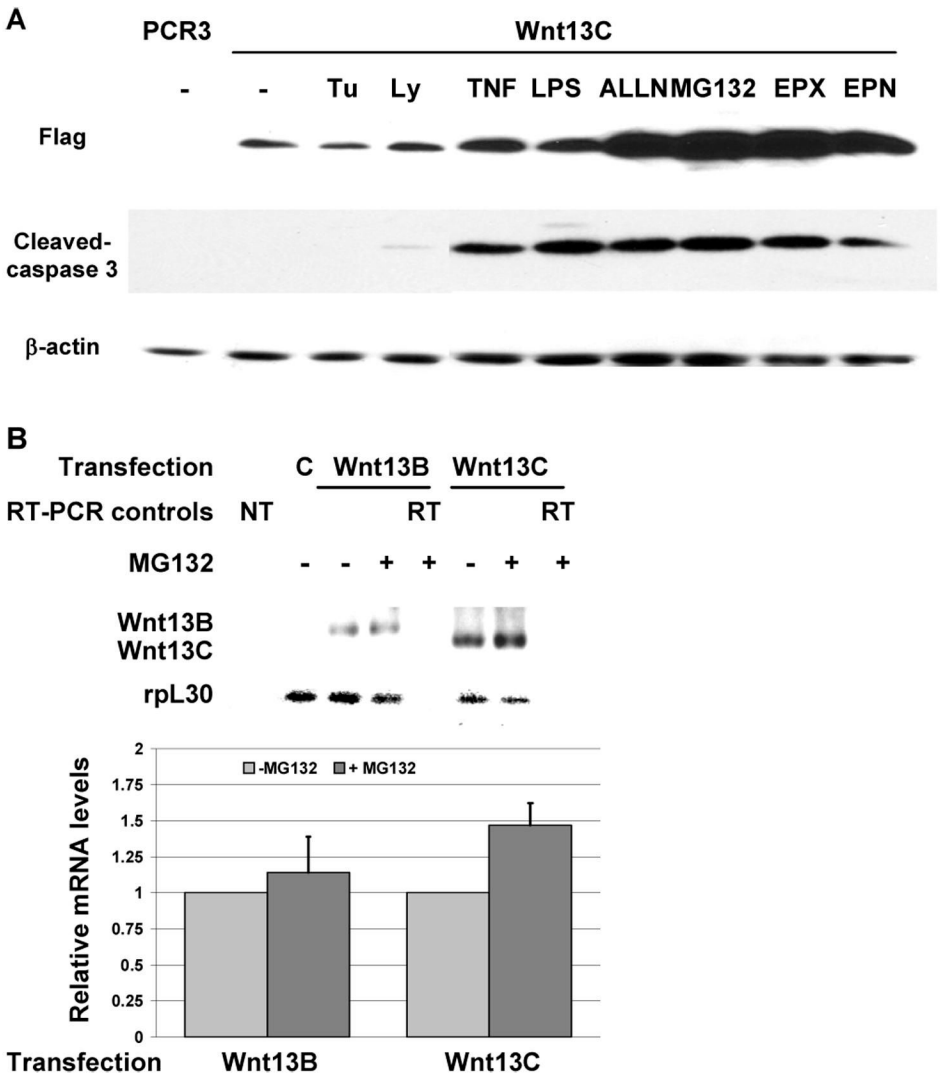

Figure 2.

The expression of Wnt13C increased in response to stress- and apoptosis-inducing agents. A) BAEC were transfected with Wnt13C-Flag construct for 24 h prior to being treated with 100 ng/ml LPS, 10ng/ml TNFα, 2.5 μg/ml Tunicamycin (Tu), 10 μM LY294002 (LY), 25 μM ALLN, 1 μM MG132, 1 μM epoxomycin (EPX) and 1 μM eponomycin (EPN) for 16 h. Wnt13-Flag proteins and cleaved-caspase 3 were analyzed by western blotting using β-actin as loading control. C) The integrity and levels of exogenous Wnt13B-Flag and Wnt13C-Flag mRNAs in BAEC treated with (+) or without (−) 1 μM MG132 were analyzed on 2% agarose gels along with the no template (NT) PCR control and minus reverse transcriptase (−RT) control, and quantified by real time PCR respectively. The relative mRNA levels after normalization are represented in the graph (mean ± SEM, n=3 independent transfection experiments).

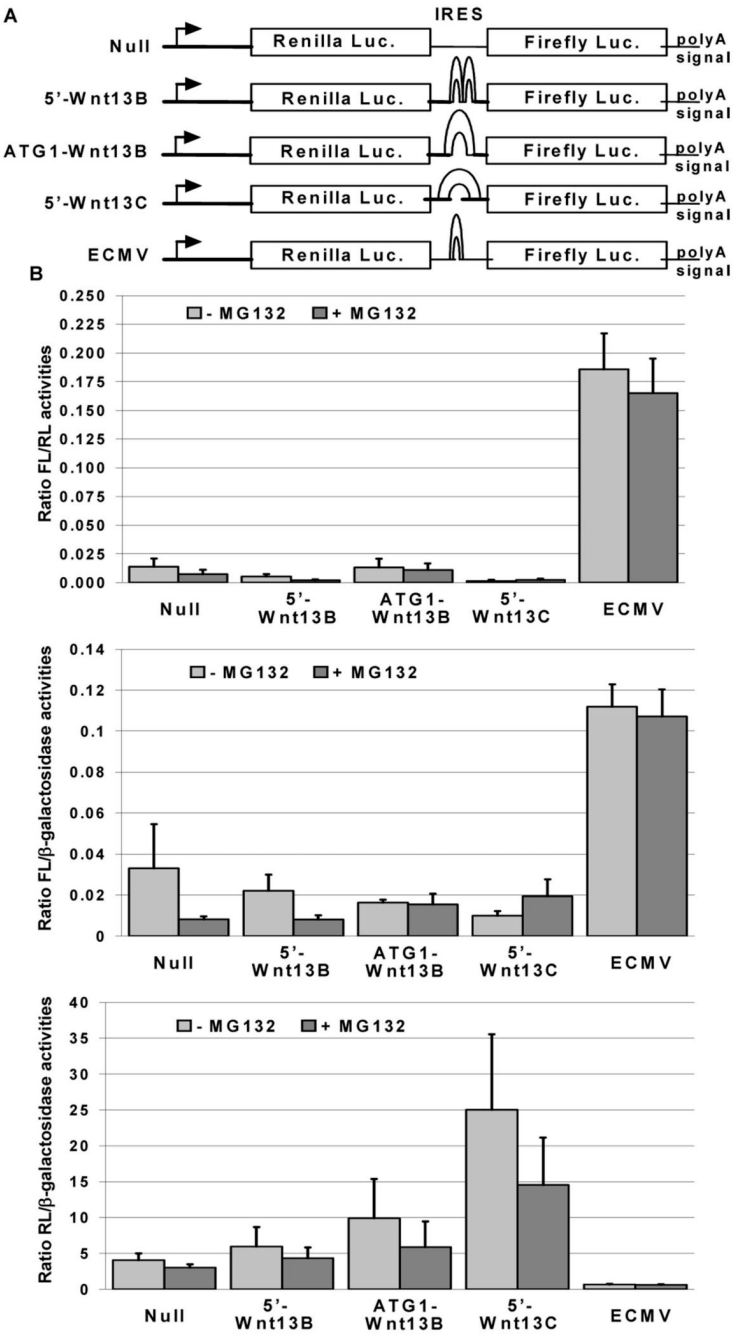

Figure 3.

The 5'-RNA leaders of Wnt13B and Wnt13C do not exhibit an IRES activity. HEK293 cells were co-tranfected with pCMV-β-galactosidase and with the dicistronic pRL-FL constructs schematically represented (A) for 24 h prior to being treated with (+) or without (−) 1 μM MG132 for an additional 10 h period. After cell lysis, the RL, FL and β-galactosidase activities were determined (B). The results are presented as the mean ± SEM of the ratio FL/RL activities, RL/β-galactosidase activities and FL/β-galactosidase activities obtained in 4 independent experiments.

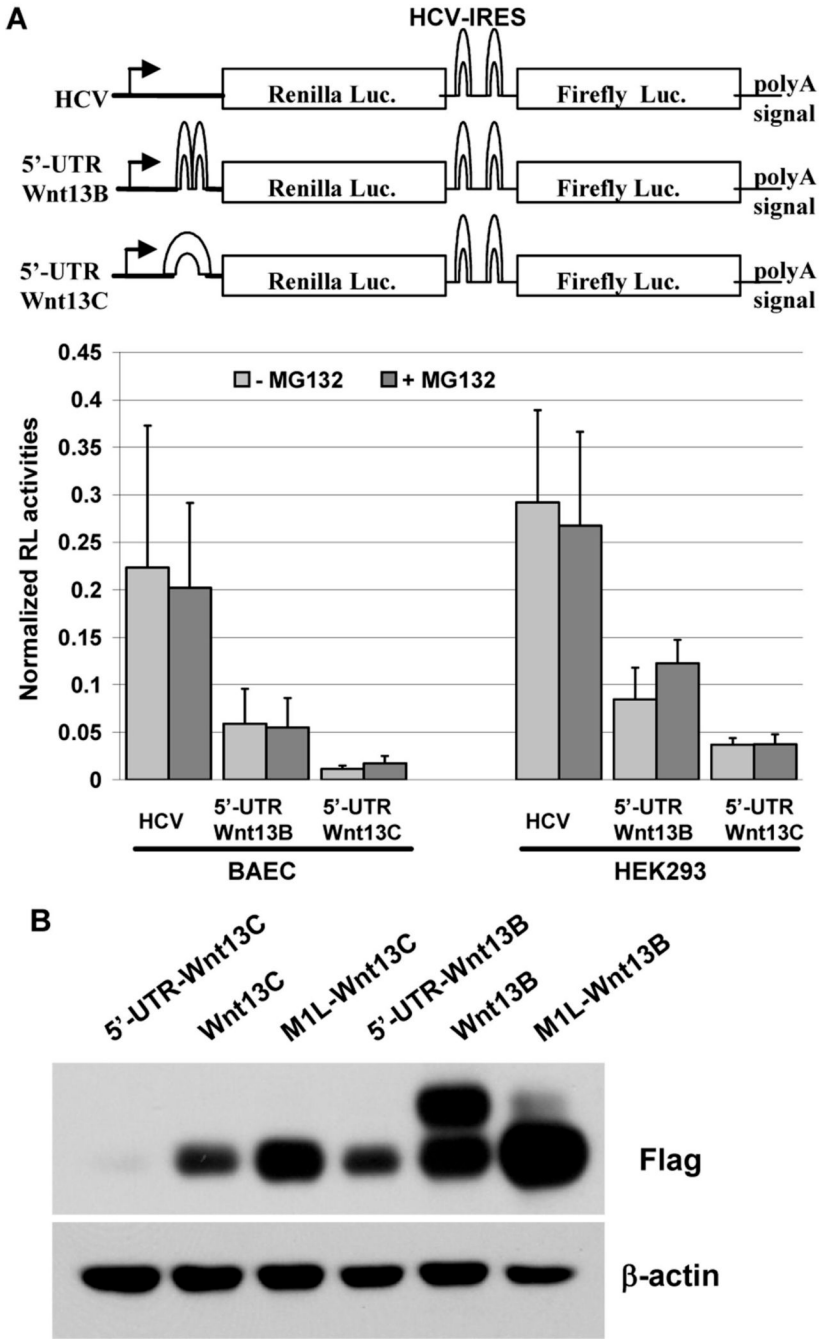

Figure 4.

The 5'-leaders of Wnt13B and Wnt13C mRNAs decrease the efficiency of translation. BAEC and HEK293 cells were transfected with pRL-HCV-FL construct as control or with p5'UTR-Wnt13B-RL-HCV-FL and p5'UTR-Wnt13C-RL-HCV-FL constructs containing the 5'-leader sequences upstream of the RL coding region with the AUG(+74) in frame with the RL start codon. After 24 h transfection, the cells were treated with vehicle (−) or 1 μM MG132 (+) for 10 h. After cell lysis, the RL, FL and β-galactosidase activities were determined. The results are presented as the mean ± SEM of the ratio RL/β-galactosidase activities obtained in 3–4 independent experiments. B) Western blot analysis of Wnt13C-Flag expression after transfection of HEK293 cells with Wnt13C-Flag and Wnt13B-Flag constructs containing

variable number of uORFs: 5’-UTR-Wnt13C (2), Wnt13C (1), M1L-Wnt13C (0), 5’-UTR-Wnt13B (1), Wnt13B and M1L-Wnt13B(0).

Table 1

Organization of Wnts 5'-UTR with the positions of the start codon and numbers of uORFs.

	Homo Sapiens			*Mus Musculus*		
Wnt	**5'UTR Exon**	**Start codon**	**uORFs**	**5'UTR Exon**	**Start codon**	**uORFs**
Wnt13A/Wnt2B2	1 → 201	20		1 → 413	238	2
Wnt13B/Wnt2B1	1 → 174	121	1			
Wnt13C	1 → 174	229	2			
Wnt1	1 → 302	199	1	1 → 436	333	1
Wnt2	1 → 377	295	2	1 → 152	70	2
Wnt3	1 → 199	120	1	1 → 125	46	1
Wnt3A	1 → 149	79	0	25 → 302	127	1
Wnt4		105	0	1 → 122	46	0
Wnt5A	1 → 324	319	0	1 → 642	637	2
Wnt6	1 → 295	216	1	1 → 331	255	1
Wnt7A	1 → 376	306	1	1 → 331	261	1
Wnt8B	1 → 185	115	0	1 → 196	132	1
Wnt9A	1 → 106	12		1 → 138	44	1
Wnt10A	1 → 576	464	1	9 → 775	663	5
Wnt10B	1 → 306	347	1	1 → 293	332	1
Wnt11	1 → 206	124	0	10 → 302	271	0
Wnt16A	1 → 352	258	2	1 → 372	278	1
Wnt16B	1 → 114	50	1			